

ENHANCED MODEL OF FOUR WAY VALVES CHARACTERISTICS AND ITS VALIDATION AT LOW TEMPERATURE

Jean-Charles Maré and Batoul Attar

Université de Toulouse, INSA - UPS, LGMT (Laboratoire de Génie Mécanique de Toulouse)
135 avenue de Rangueil, 31077 Toulouse Cedex 4, France
jean-charles.mare@insa-toulouse.fr, batoul.attar@insa-toulouse.fr

Abstract

This paper deals with the modelling of sliding spool valves that are used in hydraulic actuation systems. A new model of continuity between opened and closed orifice configurations is proposed and validated from -40 to +32 degrees Celsius. It aims at reproducing accurately the experimental pressure gain, flow gain and leakage flow for a wide range of operating temperatures in the absence of detailed knowledge of the valve design. The proposed unified model of flow at valve orifices considers the mode of operation (opened or closed orifice) and the flow conditions (laminar or turbulent) with special attention to continuity around the hydraulic null. The leakage flow in closed orifice configuration is modelled with reference to a short orifice instead of a laminar gap between infinite planes. The parameter identification and model validation processes are presented in detail and the results are displayed for an aerospace flight control servovalve.

Keywords: flow gain, hydraulic, identification, low temperature characteristics, modelling, orifice, pressure gain, servovalve, spool valve

1 Introduction

Most of the closed loop hydraulic actuators are controlled by servovalves (or proportional valves) that can significantly limit the actuator performance (Blackburn, 1960; Merritt, 1967). This effect can be split in two parts. On the one hand, the hydraulic static characteristic of the servovalve power stage alters both actuator open loop gain and pressure-flow sensitivity, limiting the closed loop accuracy, and in some cases the closed loop stability. On the other hand, the servovalve dynamics introduce amplitude and phase lag effects that influence directly the actuator open loop transfer and consequently its closed loop performance. Unfortunately, system designers suffer in practice from the lack of sufficiently accurate models of servovalves that can reproduce the effect of operating conditions on performance. The following work has been initiated by this need that was reported by different aircraft makers or aerospace equipment suppliers. Considering the main effects that are observed in practice, it is split in two parts. The first one, which is presented below, aims at reproducing the hydraulic characteristic of the power valve and its sensitivity to the operating temperature.

The second one, not addressed in this paper, is dedicated to the modelling of the servovalve dynamics, focusing especially on its electric motor and hydraulic pilot stage in order to reproduce the influence of control signal magnitude and supply pressure on its dynamics.

In very common cases like position or pressure control, the average velocity of the actuator is null. The actuator closed-loop performance and energy loss are widely influenced by the power valve static hydraulic characteristic that denotes the relation between the valve opening, its output flow and its output pressure. When modelling the actuator performance, three valve gains naturally appear: the flow-opening gain, the pressure-opening gain and the pressure-flow gain, only two of them being independent. In addition, when the valve has to operate for a long time around the null opening, e.g. for flight control actuators in cruise conditions, the valve internal leakage has also to be considered because it becomes a significant contributor to the actuator energy loss. For embedded systems applications (e.g. aerospace, ground or earth moving machinery), the hydraulic characteristic is very sensitive to the operating temperature which significantly affects some of

This manuscript was received on 13 February 2008 and was accepted after revision for publication on 30 September 2008

the fluid properties. It requires a specific effort in modelling the hydraulic fluid properties vs. temperature, the mode of operation (opened or closed orifice) and the flow pattern (laminar or turbulent) of the power valve variable orifices.

2 Modelling

The present study deals with a proportional, symmetrical, four-way, cylindrical spool valve. However, the proposed methodology and orifice model can apply without any difficulty to other types of valves. Functionally, the spool valve, Fig. 1, performs a full Wheastone bridge between the supply and return lines: the hydraulic resistances (a, c) and (b, d) vary in opposition as a function of the valve opening to drive the downstream hydraulic load.

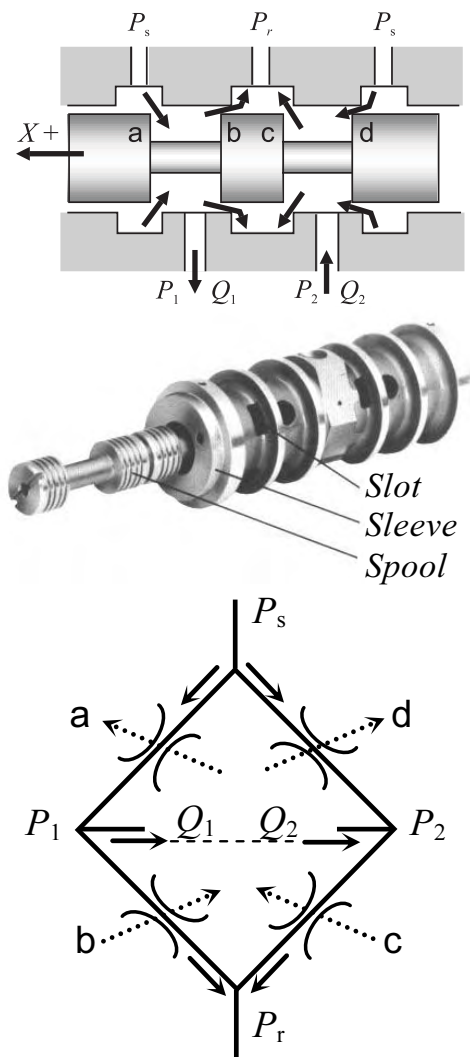


Fig. 1: Valve under study (top: schematic, centre: image, bottom hydraulic schematic)

The hydraulic null of the valve is usually defined as the opening that produces null useport flows ($Q_1 = Q_2 = 0$) when the valve is connected to the hydraulic load. In the most common case, the valve is designed symmetrically, producing $P_1 = P_2$ at hydraulic null. When associated with unloaded hydraulic motors or symmet-

rical jacks, such a design provides a symmetrical power capability that simplifies the controller design.

2.1 Fluid Hydraulic Properties

The steady-state hydraulic characteristic of a valve is significantly influenced by the fluid viscosity and density. For the Skydrol IV that is used as the hydraulic fluid on today’s commercial aircrafts, the kinetic viscosity is reduced by 66 times between $-40\text{ }^\circ\text{C}$ and $70\text{ }^\circ\text{C}$ at atmospheric pressure while the density decreases by 8.5 %. At $10\text{ }^\circ\text{C}$, the viscosity is doubled between 0 MPa and 30 MPa relative pressures (SAE, 2000).

This demonstrates the importance of reproducing these changes with accuracy to predict the valve performance over a wide domain of operating temperatures. A parametric model is preferred to tabulated data as it can force by design the consistency between physical properties, especially between specific volume and Bulk modulus. For this reason, a fluid model has been developed by the authors within the AMESim environment (AMESim, 2004) from the data provided in the SAE information report 1362 (SAE, 2000). It allows the calculation of all physical properties from four independent physical properties (specific volume v , thermal conductivity λ_c , dynamic viscosity μ and specific heat at constant pressure C_p) given at operating temperature and pressure. For density, the model of the specific volume v , Eq. 1, introduces a maximum relative error of 0.12 %. When it is combined with the model of the dynamic viscosity, Eq. 2, the modelling error on the kinetic viscosity remains below 7 cst, leading to a maximum relative error of 30 % at 0 MPa (atmospheric pressure) and $10\text{ }^\circ\text{C}$. Most of this latest error is due to the inconsistency of the data provided in (SAE, 2000).

$$v = v_0(1 + a_p \Delta P + a_{p2} \Delta P^2 + a_t \Delta T + a_{t2} \Delta T^2 + a_{pt} \Delta P \Delta T) \tag{1}$$

$$\mu = \mu_0 10^{(b_p \Delta P + b_t \Delta T + b_{t2} \Delta T^2)} \tag{2}$$

with $a_p = -7.33 \cdot 10^{-10} \text{ Pa}^{-1}$, $a_{p2} = 3.22 \cdot 10^{-18} \text{ Pa}^{-2}$, $a_t = 8.02 \cdot 10^{-4} \text{ }^\circ\text{C}^{-1}$, $a_{t2} = 6.22 \cdot 10^{-7} \text{ }^\circ\text{C}^{-2}$, $a_{pt} = -5.44 \cdot 10^{-12} \text{ Pa}^{-1} \cdot \text{ }^\circ\text{C}^{-1}$, $b_p = 4.45 \cdot 10^{-9} \text{ Pa}^{-1}$, $b_t = -1.62 \cdot 10^{-2} \text{ }^\circ\text{C}^{-1}$ and $b_{t2} = 9.62 \cdot 10^{-5} \text{ }^\circ\text{C}^{-2}$.

2.2 Valve Opening

Orifice in opened configuration

In opened orifice configuration, the individual orifice flow is well modelled using the general orifice model, Eq. 3, in which the absolute function depicts back-flowing conditions:

$$Q = C_q S \sqrt{\frac{2}{\rho} |\Delta P|} \text{sgn}(\Delta P) \tag{3}$$

When the Reynolds number is well below a few hundred, the flow is proportional to the pressure drop. The flow coefficient is then proportional to the square root of the Reynolds number, corresponding to a laminar flow as described by the Hagen-Poiseuille theory. When the Reynolds numbers increases well over typi-

cally 500, the flow coefficient tends to a constant value $C_{q\infty}$ that is representative of turbulent flow conditions. When combined, these limits define the asymptotic model of the flow coefficient (Viersma, 1980).

In practice, the flow can be influenced by additional effects such as transient flow, direction of flow, reattachment and cavitation. However, in the particular case of aerospace servovalves, these effects are generally negligible.

In order to avoid any algebraic loop when calculating the orifice flow from its pressure drop, the flow number λ is preferred to the Reynolds number (Beck, 1967):

$$\lambda = \frac{D_h}{\nu} \sqrt{\frac{2}{\rho} |\Delta P|} \quad (4)$$

where

$$Re = C_q \lambda \quad (5)$$

The dependency of the flow coefficient to the flow number is commonly represented by a hyperbolic tangent function Eq. 6, that smoothes the transition between laminar and turbulent flow conditions.

$$C_q = C_{q\infty} \tanh\left(\alpha \frac{\lambda}{\lambda_t}\right) \quad (6)$$

In addition, a detailed modelling of the valve geometry is used to describe the evolution of the orifice area versus the valve opening. In the particular case of cylindrical spool valves, Lebrun (Lebrun, 1986) showed that it was necessary to consider both radial clearance and rounded edges radius in combination with Eq. 6, Fig. 2, to obtain a hydraulic characteristic consistent with the experimental flow gain, pressure gain and leakage flow. Therefore, if the spool-bushing clearance, the slots number and width, the rounded edge radius, the transition flow number, the limit flow coefficient and the overlap are assumed to be identical for all variable orifices, the proposed spool valve model involves seven parameters (X_{i0} , r , c , n , w , $C_{q\infty}$, λ_t).

Orifice in closed configuration

There are many flow models proposed for closed configuration, but only a very few number are able to reproduce the pressure gain and the leakage characteristics. Ellman (Ellman, 1995) and (Ellman, 1998) assimilate the flow passage to a small gap within a short annulus and assume laminar conditions. The two parameter model of Eq. 7 is validated at a given temperature for a MOOG D631-236 servovalve:

$$Q = \frac{k_2}{2} \left[\sqrt{\left(\frac{k_2}{k_1}\right)^2 X^2 + 4\Delta P} - \frac{k_2}{k_1} X \right] \quad (7)$$

In another approach, Eryilmaz (Eryilmaz, 2000) considers a turbulent flow being inversely proportional to the valve closure that is also validated at a single temperature for a Moog 760-723A servovalve.

$$Q = k_1 \sqrt{\Delta P} \left(\frac{X_0^2}{X_0 - k_2 X} \right) \quad (8)$$

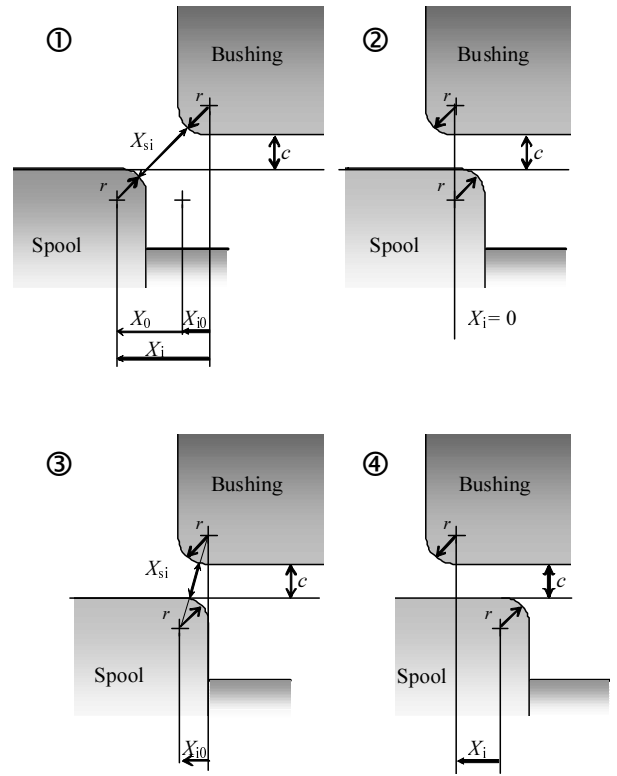


Fig. 2: Schematic of a variable orifice vs. modes of operation (Lebrun, 1986), ① opened, ② critical, ③ zero opening, ④ closed

Even if these models ensure a smooth transition between opening and closure, they cannot reproduce the effect of operating temperature that would require the modification of their parameters k_1 and k_2 accordingly.

A more physical model is proposed by Rabbie (Rabbie et al., 1981) where the flow passage is assimilated to a small gap between two infinite planes, Eq. 9:

$$\Delta P = \frac{12\mu X}{nwc^3} \left(1 + K_c + K_t \frac{c}{X} Re \right) Q \quad (9)$$

leading to the opposite causal form, Eq. 10:

$$Q = \frac{nwc^3}{12\mu(K_g + |X|)} \Delta P \quad (10)$$

Continuity between orifice opening and closure flow models is ensured through the parameter K_g that can be calculated by Eq. 11 if the flow remains laminar at null opening (Maré, 1993).

$$K_g = \frac{c(w+c)}{48\delta_\lambda w} \approx \frac{c}{48\delta_\lambda} \quad (11)$$

In practice, this assumption is not necessary if δ_λ is replaced by λC_q , as implemented in some simulation software (e.g. AMESim, 2004). However, it requires the calculation of the continuity parameter for each orifice and at each integration step.

In the present work, a new model is proposed with the following two objectives. First, it aims at reproducing accurately the valve hydraulic characteristic, whatever the operating temperature. Second, it must use a simple and generic model based on Eq. 3 without increasing the number of parameters to be identified.

In this attempt, the flow in closed orifice configura-

tion is assimilated to the flow through a short orifice instead of a small gap between infinite planes. The corresponding flow coefficient is taken from Merritt (Merritt, 1968) as a function of DRe / L . The short orifice length L is associated with the valve orifice closure $|X|$ while the short orifice diameter is associated with the hydraulic diameter of the flow passage D_h , Eq. 12 and Eq. 13.

$$S = cnw \tag{12}$$

$$D_h = 2wc / (w + c) \tag{13}$$

When $D_h Re / |X| < 50$, it is proposed to identify the flow coefficient of Eq.3 from this short orifice model, giving

$$C_q = (2.28 + 64|X|/D_h Re)^{-1/2} \tag{14}$$

Combining this result with Eq. 4 and applying to the spool orifice in closed conditions gives the flow coefficient limit for large closures as

$$\lim_{|X| \rightarrow \infty} C_q = D_h \lambda / 64|X| \tag{15}$$

The same process is applied when $D_h Re / |X| > 50$ which yields

$$C_q = (13.74 \sqrt{|X|/D_h Re} + 1.5)^{-1/2} \tag{16}$$

giving this time the flow coefficient limit for small orifice closures

$$\lim_{|X| \rightarrow 0} C_q = 1/\sqrt{1.5} = 0.816 \tag{17}$$

It results from this closed orifice modelling approach that when $|X|$ increases from null, the flow coefficient starts with a constant value then becomes progressively proportional to $\lambda / |X|$. According to this, a model, Eq. 18, is proposed to reproduce the evolution of the flow coefficient under closed orifice configuration:

$$C_{qi} = C_{q\infty} \tanh\left(\frac{\lambda_t}{\lambda_t(1 + K_g |X_i|)}\right) \tag{18}$$

with the constant ensuring continuity

$$K_g = \frac{64C_{q\infty}}{D_h \lambda_t} = \frac{32(w + c)C_{q\infty}}{wc \lambda_t} \tag{19}$$

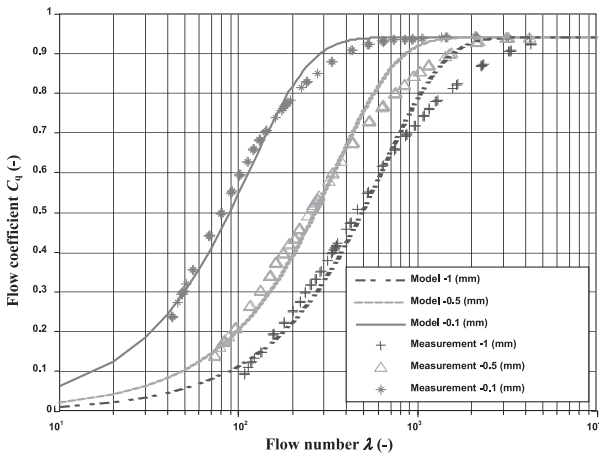


Fig. 3: Simulated flow coefficients in closed orifice configuration

The evolution of the flow coefficient with respect to valve closure and flow number is plotted on Fig. 3. The consistency of the proposed model with experimental data is proven by superposing the $C_q(\lambda)$ curves measured by Tchouprakov (Tchouprakov, 1979).

This result provides the cornerstone of the following enhanced orifice model. The general flow Eq. 4 is used whatever the valve opening. In order to ensure continuity at null opening, the product $C_q S$ must give the same value whatever the model (closed or opened orifice). The area model being already continuous, this requires the flow coefficient to be itself continuous around the null orifice opening. This condition is achieved by the proposed model of the flow coefficient that satisfies both Eq. 6 (opened orifice) and Eq. 18 (closed orifice):

$$C_{qi} = C_{q\infty} \tanh\left(\frac{\lambda_t}{\lambda_t \left[1 + \frac{1}{2} K_g (|X_i| - X_i)\right]}\right) \tag{20}$$

The continuity of the model around the critical configuration is illustrated on the 3D plot of Fig. 4.

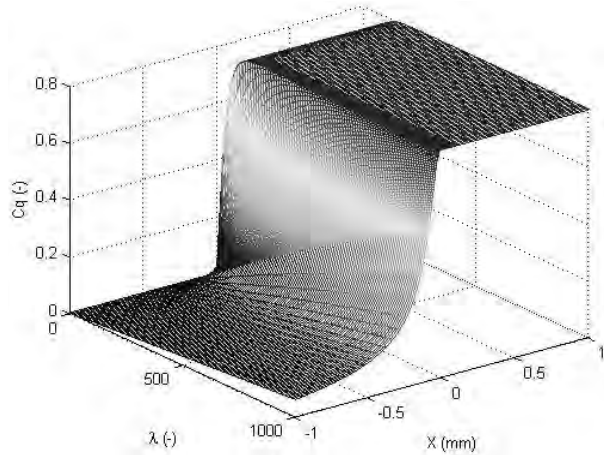


Fig. 4: Simulated flow coefficient vs. flow number and valve opening

No difference is made between orifice opening and closure for $C_{q\infty}$ and λ_t in order to reduce the number of model parameters. In that manner, there is no extra parameter in comparison with the models proposed by Lebrun (Lebrun, 1986) or Maré (Maré, 1993). However, it is possible to keep these values different by modifying Eq. 20 accordingly. The proposed orifice model is summarized in Table 1.

Table 1: Proposed 9 parameter orifice model (geometry: X_{i0} , r , c , n , w , fluid: ν and ρ , flow: $C_{q\infty}$, λ_i)

Orifice i opening $X_i = X_{i0} + \varepsilon X$
If orifice opened: Orifice i typical length $X_{si} = \sqrt{X_i^2 + (2r + c)^2} - 2r$
else orifice closed or critical: Orifice i typical length $X_{si} = c$
Orifice i area $S_i = nwX_{si}$
Orifice i hydraulic diameter $D_{hi} = 2wX_{si} / (w + X_{si})$
Flow number at orifice i $\lambda_i = \frac{D_{hi}}{\nu} \sqrt{\frac{2}{\rho} \Delta P_i }$
Orifice i flow coefficient $K_g = \frac{64C_{q\infty}}{D_h \lambda_i} = \frac{32(w+c)C_{q\infty}}{wc\lambda_i}$ (constant)
$C_{qi} = C_{q\infty} \tanh \left(\frac{\lambda_i}{\lambda_i} \frac{1}{\left[1 + \frac{1}{2} K_g (X_i - X_i) \right]} \right)$
Orifice i flow $Q_i = C_{qi} S_i \sqrt{\frac{2}{\rho} \Delta P_i } \text{sgn}(\Delta P_i)$

3 Parameter Identification and Model Validation

The proposed model has been identified and validated using the measurements taken from an aerospace servovalve equipping a recent commercial aircraft flight control actuator.

3.1 Measurements

The measurement data have been collected as specified in SAE ARP490-1 (SAE, 1993). The servovalve and inlet temperature sensor were installed inside a climatic chamber that controlled the ambient temperature T_a . All other sensors were placed outside the climatic chamber. The fluid temperature T_f was regulated through a fluid conditioning unit installed on the supply line. Low flow measurements (leakage flow and useports flow under low input current) were taken using a low friction and leakage-free piston while high flow measurements (at high input current) involved a turbine flowmeter. Both techniques ensured a 1 % reading accuracy. Pressure, temperature and current measurements were performed with a respective accuracy of 0.2 % full scale, 2 % reading and 0.5 % reading. Measurements were taken at three different fluid/ambiance temperatures. A post processing was applied to all data, firstly by a low-pass filter using a Savitzky-Golay acausal weighted moving average (Gander, 1997) then by oversampling to reduce the data file size. The servovalve pilot stage being not supplied sepa-

rately, the servovalve leakage measurements included the pilot stage consumption. Consequently, the spool valve leakage flow of the spool valve under study was extracted from these data, assuming the pilot stage consumption was constant under static operation (Faisandier, 2006).

3.2 Methodology

The first step is dedicated to the identification of the model parameters from the three types of hydraulic characteristics (flow gain plot, pressure gain plot and leakage plot). The vector of unknown parameters is determined using a curve-fitting approach that is run for the medium temperature measurements ($T_f = -15$ °C, $T_a = -40$ °C). In this attempt, a least squares method is implemented in the *MS-Excel* environment taking benefit of its *solver* tool. This low-cost solution allows any user to run the identification process without dependence on specialized and expensive software.

The second step aims at validating the model. The parameters identified in the first step are used to predict the hydraulic characteristics for other operating temperatures ($T_f = 32$ °C, $T_a = 24$ °C and $T_f = -40$ °C, $T_a = -55$ °C). These outputs are then compared with experimental data to prove the model's ability to predict the valve static hydraulic characteristic over the considered temperature range.

3.3 Parameters Identification

In Maré (Maré, 1993), the identification process was applied to a MOOG 76101 servovalve at constant operating temperature, without assuming the same overlap at hydraulic null. This allowed the reproduction of the effective useports pressures at hydraulic null that is often lower than the mean supply pressure $(P_s + P_r)/2$ in order to reduce the external leakage and steady mean static pressure at the hydraulic load. This is performed by setting a greater underlap on slots to the return line (ports b and d on Fig. 1) than on slots from the supply line (ports a and c). For this reason, individual orifice overlaps are also identified in this work.

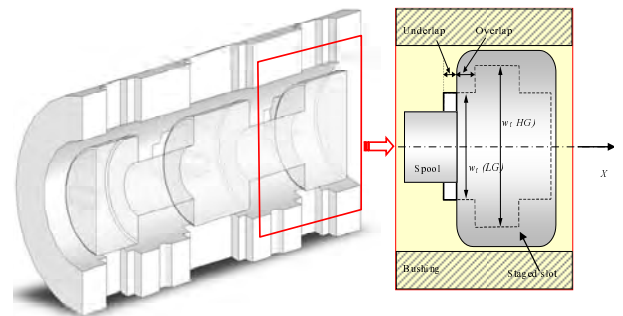


Fig. 5: Staged slots spool valve

In the present study, the flow/opening characteristic of the valve has two functional slopes. Under 25 % X_n , the low flow gain ensures a stable operation of the closed-loop position-controlled actuator. For greater input currents, the higher flow gain contributes to reduce the tracking error without altering stability (at large openings, the flow pressure gain of a valve provides a signifi-

cant hydraulic damping to the actuator). This is performed forming a staged slot, as illustrated by Fig. 5.

In the present study, the number of slots was supplied by the servovalve manufacturer. For the identification process, it is assumed that the spool-bushing clearance, the rounded edge diameter, the transition flow number and the limit flow coefficient are identical for all variable orifices. Consequently the parameters identification is split in two parts.

The first step concerns the identification of the low gain vector of parameters

$$\Theta_L = [X_{a0L} \ X_{b0L} \ X_{c0L} \ X_{d0L} \ w_L \ r \ c \ C_{q\infty} \ \lambda_{tL}]^T \quad (21)$$

The least squares criteria, Eq. 22, is minimised for both flow gain plot (full range), pressure gain and leakage plots (input range $[-6.25 \% X_n; 6.25 \% X_n]$ that provides rich data). The weighting coefficients R_1 and R_2 are introduced to fix the relative importance given to the reproduction of each characteristic. In practice, they are set according to the ratio between the full scales of the associated quantities.

$$J = \min_{\Theta_L} \sum_{\text{measures}} \left[\begin{aligned} &(\hat{Q}_1 - Q_1^\#)^2 + R_1 \{(\hat{P}_1 - P_1^\#)^2 + (\hat{P}_2 - P_2^\#)^2\} \\ &+ R_2 \{(\hat{Q}_2 - Q_2^\#)^2 + (\hat{Q}_3 - Q_3^\#)^2\} \end{aligned} \right] \quad (22)$$

Some Remarks: The width and number of slots are design parameters of the valve that can be easily provided by the manufacturer. Consequently, it is easy to identify from the flow gain plot at large valve openings:

- the limit value $C_{q\infty}$ of the flow coefficient that fixes the flow-opening gain if n and w are known,
- the average value of $X_{i0} + r$ that fixes the asymptotic valve opening at null flow.

The second step deals with the high gain region in which the remaining parameters are grouped in the vector Θ_H , Eq. 23. They are identified using only the flow gain plot, therefore minimizing the associated criteria, Eq. 24:

$$\Theta_H = [X_{a0H} \ X_{b0H} \ X_{c0H} \ X_{d0H} \ w_H \ \lambda_{tH}]^T \quad (23)$$

$$J = \min_{\Theta_H} \sum_{\text{measures}} \left[(\hat{Q}_1 - Q_1^\#)^2 + (\hat{Q}_2 - Q_2^\#)^2 \right] \quad (24)$$

The hydraulic characteristics resulting from this identification process are summarized in Fig. 6.

The flow gain and pressure gain plots measurements require different configurations (connected or closed useports). Between these two experiments, the valve null slightly changes, requiring the compensation of this drift in the identification process. The weighting factors have been set to give the priority to the leakage flow, the maximum value of which is predicted with a 1.8 % relative error. The maximum relative error of 31 % on the pressure/opening plot comes from the asymmetry of the measured characteristic, the cause of which has not been fixed (possibly valve manufacturing tolerances or inaccurate measurement). The flow/opening characteristic is also very well reproduced by the model as the maximum relative error remains below 3.4 % in the low gain domain and below 0.44 % in the high gain domain.

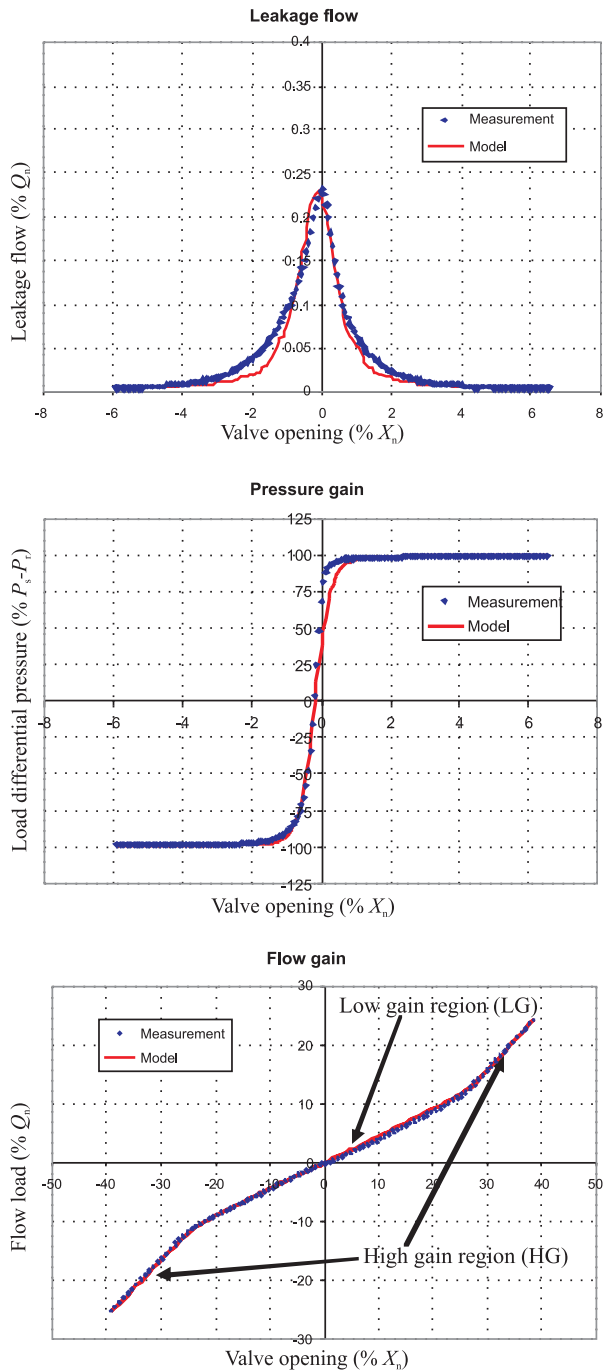


Fig. 6: Measured and simulated hydraulic characteristics used for parameters identification (-15 °C)

3.4 Model Validation

Figure 7 and Fig. 8 illustrate the model validation for lower or higher temperatures when using the parameters identified at medium temperature. Asymmetry and bias are still observed on the measurement plots. However, despite a total temperature change of 70 °C, the predicted hydraulic characteristic remains close to the measured one. Table 2 summarizes the changes versus temperature and the associated model accuracy. The worse results are obtained for the prediction of the pressure gain that is a consequence of giving the priority to the leakage accuracy in the identification process.

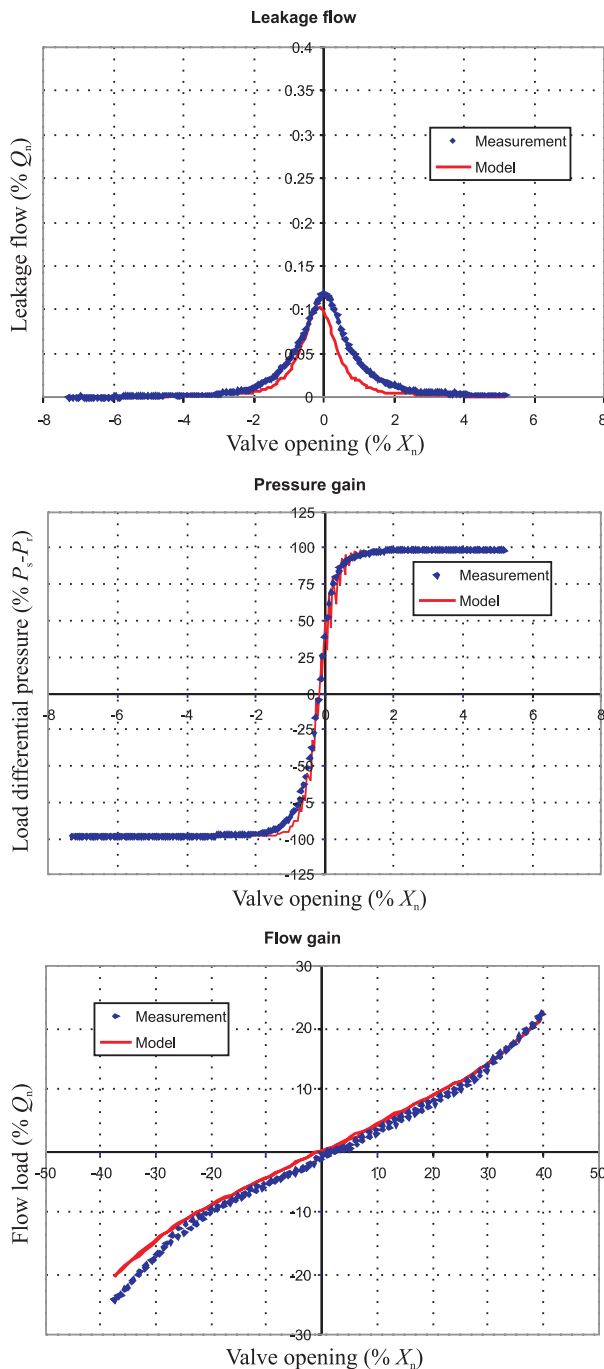


Fig. 7: Measured and simulated hydraulic characteristics at -40 °C

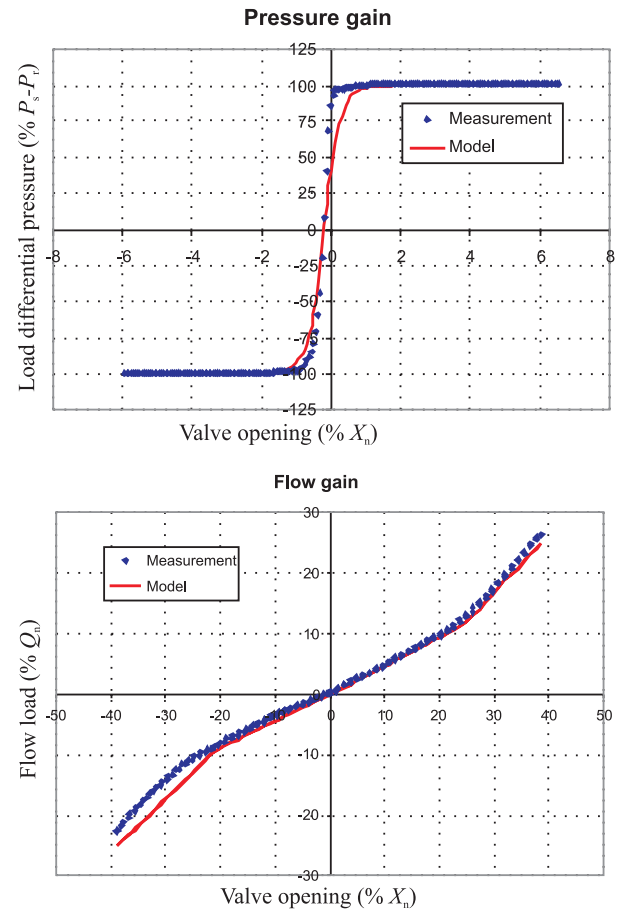
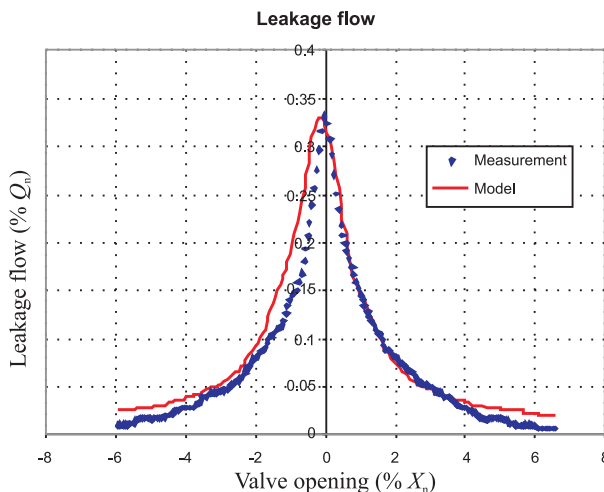


Fig. 8: Measured and simulated hydraulic characteristics at 32 °C

Table 2: Model performance over temperature changes

Fluid temperature	-40 °C	-15 °C	+32 °C
Maximum leakage			
Measured (% Q_n)	0.12	0.23	0.33
Change from -15 °C	-48 %	-	+44 %
Model relative error (%)	-12.36 %	-1.82 %	-0.93 %
Pressure gain			
measured over ± 0.25 % X_n			
Measured (% P_s / % X_n)	202	300	381
Change from -15 °C	-34 %		+27 %
Model relative error	-2 %	-31 %	-45 %
Pressure gain			
measured over ± 40 % P_s			
Measured (% P_s / % X_n)	209	319	481
Change from -15 °C	-34 %		+51 %
Model relative error	-24 %	-33 %	-55 %
Low flow gain			
Measured (% Q_n / % X_n)	0.48	0.46	0.49
Model relative error	+1 %	+4 %	-1 %
High flow gain			
Measured (% Q_n / % X_n)	0.85	1.02	1.03
Model relative error	-13 %	+1 %	-6 %
Useport pressure at null			
Measured (% P_s)	37.6	46.2	54.3
Change from -15 °C	-19 %		+18 %
Model relative error	+7.7 %	-15.6 %	-27.7 %

When analysing these results, it has to be kept in mind that the effective values of the fluid physical properties (especially viscosity and density) have a great influence on the predicted valve characteristics. During service, they can differ significantly from the SAE standard data that only provides reference values. In practice, a permanent loss of viscosity occurs after some hundred hours of service due to shear in valves and pumps that brakes the long molecular chains of the viscosity index additives. Recent airmaker measurements have shown that the in-house measured kinetic viscosity can be 15 % lower than the value provided by the oil supplier.

4 Conclusion

The reported work intended to provide an enhanced generic model of four-way valves in order to reproduce their hydraulic characteristic over a wide range of operating temperatures.

After developing a temperature/pressure dependant model of the fluid physical properties, special consideration was given to continuity between closed and opened orifice configurations. In this attempt, it has been suggested to assimilate the passage in closed orifice configuration to a short orifice rather than a small gap between infinite planes. This led to form a unique expression of the flow number, applicable in both closed and opened orifice configurations, without requiring an extra continuity parameter.

The interest of the proposed approach has been demonstrated for an aerospace servovalve operated at a fluid temperature of -40 °C, -15 °C and +32 °C. The mid temperature experiments have been used to identify the model parameters from a curve-fitting approach while the measurements at extreme temperatures were reserved for model validation.

Even with unexplained unsymmetrical measured data from the supplier, the comparison between simulated and experimental hydraulic characteristics proved the interest of the proposed model. As the main weighting factor was given to the valve leakage, the pressure-gain prediction was less accurate with globally underestimated values.

Nomenclature

a_{p1}	Pressure coefficient	[1/Pa]
a_{p2}	Square pressure coefficient	[1/Pa ²]
a_{t1}	Temperature coefficient	[1/°C]
a_{t2}	Square temperature coefficient	[1/°C ²]
a_{pt}	Pressure-Temperature coefficient	[1/Pa°C]
b_{p1}	Pressure coefficient	[1/Pa]
b_{t1}	Temperature coefficient	[1/°C]
b_{t2}	Temperature coefficient	[1/°C ²]
c	Spool bushing radial clearance	[m]
C_p	Specific heat at constant pressure	[J/Kg/°C]
C_q	Flow coefficient	[-]
D	Short orifice diameter	[m]
D_h	Hydraulic diameter	[m]

J	Criteria to be optimized	
k_1, k_2	Coefficients of representation model	
K_e	Loss factor at entrance	[-]
K_g	Constant to ensure continuity	[1/m]
K_t	Loss factor in transition length	[-]
n	Number of slots	[-]
P	Pressure	[Pa]
Q	Volume flow	[m ³ /s]
r	Rounded edge radius	[m]
Re	Reynolds number	[-]
R_1	Weighting coefficient	[Pa/m ³ /s]
R_2	Weighting coefficient	[-]
S	Flow area at orifice	[m ²]
T	Temperature	[°C]
w	Slot width	[m]
X	Valve opening	[m]
X_s	Orifice length	[m]
δ_λ	Limit slope of $C_q(\lambda)$	[-]
ε	Sign operator, positive if orifice opens when X increases	[-]
λ	Flow number	[-]
λ_c	Thermal conductivity	[W/m/°C]
μ	Dynamic viscosity	[Pa]
ν	Kinematic viscosity	[m ² /s]
ρ	Density	[Kg/m ³]
ν	Specific volume	[m ³ /kg]
ΔP	Pressure difference	[Pa]
ΔT	Temperature difference	[°C]
Θ	Vector of parameters	

Subscripts

a	Ambiance
a...d	Variable orifices index
f	Fluid
H	High gain region
i	Current orifice index
L	Low gain region
n	Nominal
r	Return
s	Supply
t	Transition value
0	Reference value
1, 2	Use ports index
∞	Limit value

Exponent

T	Transposed
^	Simulated
#	Measured

References

- AMESim, User Manual, Thermal-Hydraulic Library, IMAGINE Inc, Ed 4.2, September 2004
- Beck, A. and Mc Cloy, H. R. 1967. Some Cavitation Effects in Spool Valves. *Proceedings of Institution of Mechanical Engineering*, 182 Part 1, n°8. London.

- Blackburn, J. F., Reethof, G. and Shearer, J. L.** 1960. *Fluid Power Control*. New York. John Wiley & Sons.
- Ellman, A., Koskinen, K. and Vilenius, M.** 1995. Through-Flow in Short Annulus of Fine Clearance. *Proceeding of the ASME Dynamic Systems and Control Division*, Vol.7, pp. 813-821. Atlanta, USA.
- Ellman, A.** 1998. Leakage Behaviour of Four-Way Servo Valve. *The ASME Fluid Power Systems and Technology*, Vol. 5, pp. 163-167. Anaheim, CA.
- Eryilmaz, B. and Wilson, B. H.** 2000. Modeling the Internal Leakage of Hydraulic Servovalves. *International Mechanical Engineering Congress and Exposition, ASME*, Vol. DSC-69.1, pp. 337-343. Orlando, USA.
- Faisandier, J.** 2006. *Mécanismes Hydrauliques et Pneumatiques*. 9^e ed. Paris. Dunod.
- Gander, W. and Hřebíček, J.** 1997. *Solving Problems in Scientific Computing Using Maple and Matlab*. Springer. 3rd Edition.
- Lebrun, M.** 1986. *Contribution à une Aide à l'Analyse Dynamique et à la Conception de Systèmes Electrohydrauliques*. Mémoire de Doctorat d'Etat. Université Claude Bernard-Lyon I.
- Maré, J.-C.** 1993. *Contribution à la Modélisation, la Simulation, l'Identification et la Commande d'Actionneurs Electrohydrauliques*. Mémoire de Doctorat d'Etat. Université Claude Bernard-Lyon I.
- Merritt, H. E.** 1967. *Hydraulic Control Systems*. New York. John Wiley & Sons.
- Rabie, G. and Lebrun, M.** 1981. Modélisation par les Graphes à Liens et Simulation d'une Servo Valve Electrohydraulique à Deux Etages. *R.A.I.R.O Automatique Systems Analysis and Control*, Vol. 15(2), pp. 97-129.
- SAE.** 2000. Aerospace Hydraulic Fluids Physical Properties. *SAE Aerospace Information Report 1362*.
- SAE.** 1993. Electrohydraulic servovalves. *Aerospace Recommended Practices SAE-AR 490-1*.
- Tchouprakov, Y.** 1979. *Commande Hydraulique et Automatismes Hydrauliques*. Moscou. Ed. Mir.
- Viersma, T. J.** 1980. *Analysis, Synthesis and Design of Hydraulic Servosystems and Pipelines*. Amsterdam. Elsevier.



Maré Jean-Charles

Professor Maré Jean-Charles is a Mechanical Engineer from INSA Toulouse, 1982. His French Doctorat d'Etat, presented in 1993, dealt with electrohydraulic actuation. Since 1998, he has been a Professor at INSA Toulouse. His research and teaching activities are related to the design of actuation systems and components for aerospace applications.



Attar Batoul

Batoul Attar received her Master degree in Mechanical Engineering from the University of Aleppo in 1999. In 2008, she got her PhD from INSA Toulouse dealing with the modelling and simulation of servovalves under extreme operating conditions. She is currently an assistant Professor at the faculty of Aeronautics of the University of Aleppo, Syria.